# Ivonescimab combined with radiotherapy in the treatment of advanced lung adenocarcinoma with high expression of PD-L1: A case report

QI ZHOU, BO YANG, HONGYI CAI, JUN JIANG and RONG CHEN

Department of Oncology, Affiliated Hospital of Qinghai University, Xining, Qinghai 810000, P.R. China

Received April 2, 2026; Accepted August 27, 2026

DOI: 10.3892/ol.2026.15894

**Abstract.** The optimal sequencing of immunotherapy and radiotherapy in non-small cell lung cancer (NSCLC) remains unclear. The present study reports a case of advanced lung adenocarcinoma (cT4N2bM1a, stage IVa) with a programmed death-ligand 1 (PD-L1) tumor proportion score of 90% and TP53 mutation. The patient received first-line ivonescimab monotherapy (900 mg, every 3 weeks) for four cycles, achieving a partial response (47% reduction per Response Evaluation Criteria in Solid Tumors 1.1). Sequential thoracic radiotherapy (5,000 cGy/25 fractions) was then administered for consolidation. Serum tumor markers (carcinoembryonic antigen, cancer antigen 125, cytokeratin 19 fragment and neuron-specific enolase) exhibited markedly decreased levels from baseline. Grade I radiation pneumonitis occurred post-radiotherapy but resolved rapidly with low-dose glucocorticoids. At the last follow-up (8 months), the patient remained progression-free with the Eastern Cooperative Oncology Group performance status improving from 2 to 0. This case provides real-world evidence for the 'immunotherapy induction followed by radiotherapy consolidation' strategy in an individual with high PD-L1 expression. The presence of TP53 mutation may predict an enhanced synergistic response to combined immunotherapy and radiotherapy, warranting further investigation.

## Introduction

Lung cancer is the malignancy with the highest incidence and mortality rates globally (1). For patients with advanced non-small cell lung cancer (NSCLC) harboring driver gene-negative mutations, traditional platinum-based doublet chemotherapy demonstrates limited efficacy, with median survival time rarely exceeding 12 months (2). The advent of immune checkpoint inhibitors has transformed the therapeutic landscape. Ivonescimab (AK112), a novel programmed cell death protein 1 (PD-1)/vascular endothelial growth factor (VEGF) bispecific antibody, simultaneously blocks the PD-1/programmed death-ligand 1 (PD-L1) immune checkpoint pathway and inhibits VEGF-mediated tumor angiogenesis, exhibiting synergistic antitumor potential (3). Phase III clinical trials of ivonescimab (for example, the AK112-301 and HARMONi-A trials) demonstrated superior survival benefits over conventional chemotherapy in advanced NSCLC, particularly among populations with high PD-L1 expression (4-6). Radiotherapy not only directly kills tumor cells but also alters the tumor microenvironment, creating an 'abscopal effect' with immunotherapy. However, two key issues remain unresolved: i) The real-world efficacy dynamics of ivonescimab in the 'super-dominant population' with a PD-L1 tumor proportion score (TPS) ≥90%; and ii) the optimal timing and synergistic mechanisms for sequential radiotherapy after immunotherapy. The present study reports a case of advanced lung adenocarcinoma with a PD-L1 TPS of 90% and concurrent TP53 mutation, in which the patient achieved a sustained response after sequential radiotherapy following ivonescimab-induced monotherapy, providing preliminary clinical evidence for these issues.

## Case report

*Patient basic information and chief complaint.* A 54-year-old female farmer presented to the Affiliated Hospital of Qinghai University (Xining, China) in January 2025 with the symptoms of chest tightness, dyspnea and chest pain that had persisted for 1 month, with exacerbation over the past 5 days.

*Presenting history.* The patient developed a persistent stabbing pain in the right thoracic and back region without apparent cause at the end of January 2025, with a numerical pain rating scale (NRS) score of 6 (7). Symptoms markedly worsened after physical exertion, accompanied by progressively worsening dyspnea and nocturnal paroxysmal dyspnea requiring orthopnea, as well as a dry cough, palpitations and hyperhidrosis. In mid-January 2025, a chest computed tomography (CT) scan performed at an external hospital revealed a mediastinal mass with multiple right lung metastases, massive right

*Correspondence to:* Dr Jun Jiang or Dr Rong Chen, Department of Oncology, Affiliated Hospital of Qinghai University, 29 Tongren Road, Chengxi, Xining, Qinghai 810000, P.R. China
E-mail: xnrheum@126.com
E-mail: 18697149730@163.com

*Key words:* ivonescimab, lung adenocarcinoma, radiotherapy, immunotherapy, programmed death-ligand 1, first-line therapy

pleural effusion, interstitial lung disease with inflammation in both lungs and localized bilateral pleural thickening.

*Medical history and personal history*. The patient had no smoking history or drug allergy history, with a declared allergy to seafood.

*Physical examination*. The patient's body temperature was 36.1˚C, pulse rate was 78 beats/min, respiration rate was 16 breaths/min, blood pressure was 124/82 mmHg and body surface area was 1.5 $m^2$. The Eastern Cooperative Oncology Group performance status (ECOG PS) score was 2 (8). A physical examination of the chest revealed reduced right thoracic expansion compared with that on the contralateral side, with absent breath sounds in the right lung.

*Diagnostic evaluation*. To establish a definitive diagnosis, the patient underwent a series of examinations.

*Imaging findings*. Chest CT performed on day 22 after the initial presentation (Fig. 1) revealed the following: i) An irregular soft-tissue mass was observed in the dorsal segment of the right lower lobe, suggestive of central lung cancer (cT4 stage), accompanied by adjacent obstructive pneumonia; ii) multiple nodules of varying sizes were present in both lungs, indicating intrapulmonary metastasis (M1a) according to the eighth edition of the TNM staging system (9); and iii) multiple enlarged lymph nodes were detected in the mediastinum and right hilar region, suggesting lymph node metastasis (N2) (9).

*Systemic examination*. No definitive metastatic signs were observed on cranial magnetic resonance imaging with contrast enhancement, pelvic CT, or whole-body bone scintigraphy. Abdominal CT revealed a small cyst in the S4 segment of the liver and bilateral renal cysts.

*Pathological diagnosis*. Percutaneous lung biopsy guided by CT revealed a poorly differentiated non-small cell carcinoma.

The biopsy specimen was fixed in 10% neutral-buffered formalin at room temperature (~25˚C) for 12-24 h, processed through graded alcohols, cleared in xylene and embedded in paraffin wax. Serial sections were cut at a thickness of 4 $\mu$m and mounted on poly-L-lysine-coated glass slides. For immunohistochemical staining, sections were deparaffinized in xylene and rehydrated through graded ethanol. Antigen retrieval was performed using citrate buffer (pH 6.0) at 95˚C for 20 min in a water bath. Endogenous peroxidase activity was blocked by incubation with 3% hydrogen peroxide in methanol at room temperature for 10 min. Non-specific binding was blocked by incubation with 5% normal goat serum (cat. no. ab7481; Abcam) at room temperature for 30 min. The sections were then incubated with primary antibodies at 4˚C overnight in a humidified chamber. The primary antibodies used were as follows: Pan-CK (clone AE1/AE3; cat. no. ab27976; 1:200; Abcam), CK7 (clone OV-TL 12/30; cat. no. ab9021; 1:100; Abcam), thyroid transcription factor-1 (clone 8G7G3/1; cat. no. M3575; 1:100; Dako; Agilent Technologies, Inc.), napsin A (clone IP64; cat. no. MCA2119; 1:200; Bio-Rad Laboratories, Inc.), p40 (clone BC28; cat. no. ab202493; 1:200; Abcam), p63 (clone D2K8X; cat. no. 13540; 1:200; Cell Signaling Technology, Inc.), SMARCA4/BRG1 (clone EPNCIR111A; cat. no. ab110641; 1:100; Abcam), synaptophysin (clone DAK-SYNAP; cat. no. M0776; 1:100; Dako; Agilent Technologies, Inc.) and Ki-67 (clone MIB-1; cat. no. M7240; 1:100; Dako; Agilent Technologies, Inc.). After washing with phosphate-buffered saline, the sections were incubated with horseradish peroxidase-conjugated goat anti-rabbit or anti-mouse secondary antibody (cat. nos. ab205718 and ab205719; 1:200; Abcam) at room temperature for 30 min. Immunoreactivity was visualized using 3,3'-diaminobenzidine chromogen (cat. no. ab64238; Abcam) for 2-5 min at room temperature, followed by counterstaining with Mayer's hematoxylin for 1 min. The sections were then dehydrated, cleared and coverslipped with mounting medium. All stained sections were examined under a light microscope, and images were captured at x400 magnification.

*Molecular pathology testing*. Next-generation sequencing (NGS) was conducted on formalin-fixed paraffin-embedded (FFPE) tumor tissue obtained from the CT-guided percutaneous lung biopsy. DNA was extracted using a laboratory-developed solid tumor gene panel FFPE extraction kit, and libraries were prepared using a laboratory-developed test (LDT) solid tumor gene panel library preparation kit. Sequencing was performed on an Illumina NovaSeq 6000 platform with 150-bp paired-end reads.

Raw reads were preprocessed using Fastp (version 0.21.0; OpenGene; URL: https://github.com/OpenGene/fastp) to remove adapter sequences and low-quality bases, with quality control assessed using FastQC (version 0.11.9; Babraham Bioinformatics; http://www.bioinformatics.babraham.ac.uk/projects/fastqc/). Clean reads were aligned to the GRCh37/hg19 reference genome using BWA-MEM (version 0.7.17; Li H; URL: http://bio-bwa.sourceforge.net). PCR duplicates were removed using Samblaster (version 0.1.24; Gregory Faust; https://github.com/GregoryFaust/samblaster). Variant calling was performed using a custom in-house algorithm integrating Pisces (version 5.3.0.0; Illumina; https://github.com/Illumina/Pisces) and GATK (version 4.0.4.0; Broad Institute; https://github.com/broadinstitute/gatk/releases). Variant filtering criteria included a variant allele frequency (VAF) >1.3%, a mean sequencing depth >500x, and specific SNP/InDel depth >50x. Functional annotation was performed using a custom pipeline integrating Annovar (version 2022-01-13; Wang K; https://annovar.openbioinformatics.org), VEP (version 111.0; Ensembl; https://useast.ensembl.org/info/docs/tools/vep/index.html) and SnpEff (version 5.3; Cingolani P; https://github.com/snpEff/snpEff).

PD-L1 expression was evaluated as the TPS, defined as the percentage of tumor cells showing partial or complete membranous staining at any intensity. A TP53 missense mutation was identified, and no driver gene mutations were detected for EGFR, ALK or ROS1.

*Clinical diagnosis*. The final diagnosis was adenocarcinoma of the middle and lower lobes of the right lung (cT4N2bM1a, stage IVa), according to the eighth edition of the TNM staging system (9). with pulmonary metastasis, multiple lymph node metastases in the mediastinum and hilar region, and malignant pleural effusion.

*Treatment process and efficacy evaluation*. The patient's treatment plan was developed through multidisciplinary team discussions. The timeline of diagnosis and treatment is summarized in Table I.

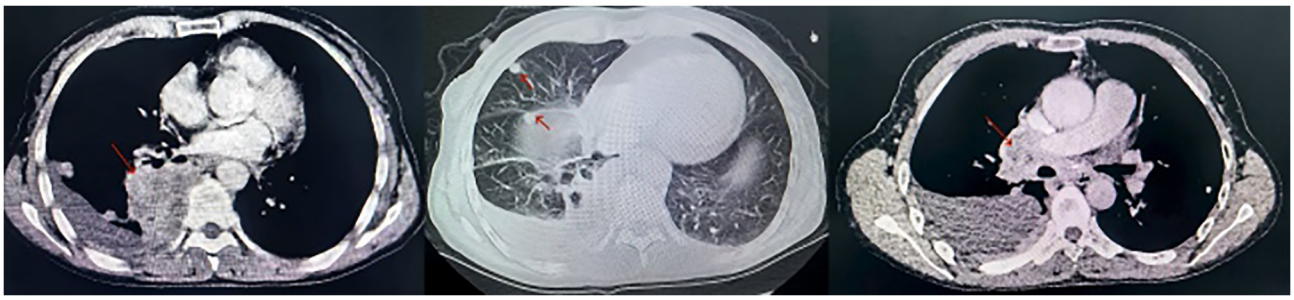


Figure 1. Baseline chest computed tomography (CT) performed on day 22 after initial presentation. Left panel (mediastinal window): Mediastinal window showing the primary tumor in the dorsal segment of the right lower lobe (arrow), ~6.5 cm in longest diameter. Middle panel (lung window): Lung window demonstrating multiple intrapulmonary metastatic nodules in the right lung (arrows). Right panel (mediastinal window): Mediastinal window revealing massive right pleural effusion and the primary lesion (arrow). Scanning parameters: 120 kV, 150 mAsec, 5-mm slice thickness. Scale bar, 1 cm.

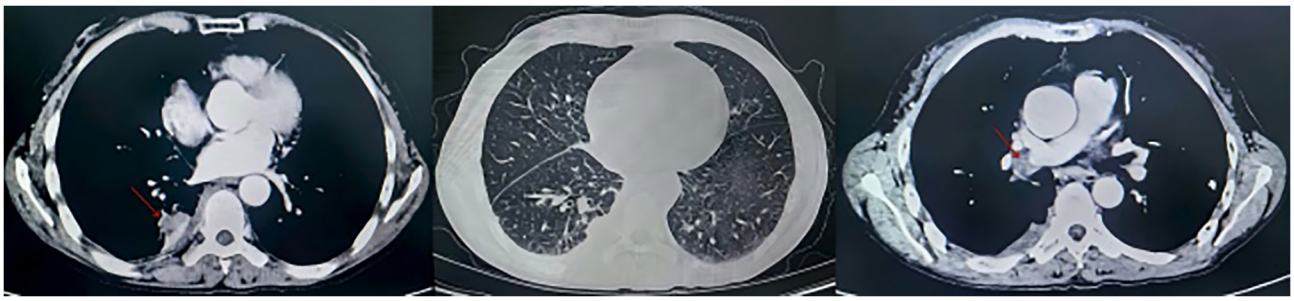


Figure 2. Chest computed tomography after 2 cycles of ivonescimab (April 2025), demonstrating a partial response (33% reduction in target lesions per RECIST 1.1). Left panel: Notable reduction of the primary tumor with near-complete resolution of pleural effusion (arrow). Middle panel: Marked improvement of intrapulmonary metastases. Right panel: Near-complete resolution of pleural effusion. Scanning parameters: 120 kV, 150 mAsec, 5-mm slice thickness. Scale bar, 1 cm.

*Initial supportive therapy and local treatment (February 2025).* The patient was admitted to the Affiliated Hospital of Qinghai University with concurrent pulmonary infection and massive right-sided pleural effusion. Empirical anti-infective therapy with levofloxacin (500 mg once daily for 7 days) was administered, followed by closed thoracic drainage, resulting in symptom relief. To control the pleural effusion, three intrapleural perfusion treatments of 60 mg cisplatin + 200 mg bevacizumab were performed on days 1, 6 and 9 of the intrapleural perfusion regimen. Post-treatment, the pleural effusion was well controlled.

*Systemic immunotherapy (February to June 2025).* Based on the patient's high PD-L1 expression status, ivonescimab (AK112) was initiated as monotherapy on day 6 of the intrapleural perfusion regimen (concurrent with the second intrapleural perfusion), at a dose of 900 mg administered intravenously every 3 weeks. The treatment course proceeded smoothly.

*Efficacy evaluation.* Baseline imaging performed on day 22 after initial presentation is shown in Fig. 1. Chest enhanced CT re-examination was performed after two cycles of treatment (April 2025) (Fig. 2) and four cycles of treatment (June 2025) (Fig. 3). Percutaneous lung biopsy guided by CT revealed a poorly differentiated non-small cell carcinoma (Fig. 4A and B). Immunohistochemical staining results were as follows: Thyroid transcription factor-1 (+) (Fig. 4C), napsin A (+) (Fig. 4D), tumor protein p40 (-) (Fig. 4E), tumor protein p63 (-) (Fig. 4F), pan-cytokeratin (pan-CK) (+) (Fig. 4G), CK7 (+) (Fig. 4H), SMARCA4/BRG1 (-) (Fig. 4I), synaptophysin (-) (Fig. 4J) and a Ki-67 proliferation index ~70% (Fig. 4K). These findings supported a diagnosis of pulmonary adenocarcinoma. According to the Response Evaluation Criteria in Solid Tumors 1.1, both assessments demonstrated a partial response (PR). Specifically, the sum of the longest diameters of the target lesions decreased by 33 and 47%, respectively, compared with baseline. The dynamic changes in serum tumor markers are shown in Table II, with marked reductions in carcinoembryonic antigen (CEA), carbohydrate antigen 125 (CA125), cytokeratin 19 fragment (CYFRA21-1) and neuron-specific enolase (NSE) levels compared with pre-treatment levels. Notably, SCC remained within the normal range throughout the treatment course.

*Sequential radiotherapy (June to July 2025).* Based on achieving a good response to systemic therapy, sequential chest radiotherapy was initiated in June 2025 to consolidate local lesion control. Intensity-modulated radiotherapy was employed, with the following target volumes defined: Gross tumor volume 1 (GTV1) was the imaging-confirmed primary lesion in the right lung, with a prescription dose of 1,000 cGy/5 fractions; and GTV2 included the right lung metastatic lymph nodes and high-risk lymphatic drainage prophylaxis areas, with a prescription dose of 5,000 cGy/25 fractions. The radiotherapy plan was successfully completed.

*Management and follow-up of adverse events.* Approximately 20 days after radiotherapy (end of July 2025), a follow-up CT scan revealed stable primary lesions but new ground-glass opacities and linear opacities in the lungs, suggestive of radiation

Table I. Timeline of diagnosis and treatment.

| Date | Action |
|---|---|
| January 2025 | Diagnosis (cT4N2bM1a, stage IVa) |
| February 2025 | Intrapleural perfusion (60 mg cisplatin + 200 mg bevacizumab) on days 1, 6 and 9; each instilled via chest tube, clamped for 2 h with positioning |
| February-June 2025 | Ivonescimab monotherapy (900 mg every 3 weeks for four cycles) |
| April 2025 | PR after two cycles |
| June 2025 | June 2025: PR after four cycles (47% reduction) |
| June-July 2025 | Sequential thoracic radiotherapy (5,000 cGy/25 fractions) |
| Late July 2025 | Grade I radiation pneumonitis, resolved with steroids |
| August 2025 | Last follow-up: PFS, 8 months; ECOG PS, 0 |

PR, partial response; PFS, progression-free survival; ECOG, Eastern Cooperative Oncology Group performance status.

Table II. Dynamic changes in serum tumor markers with normal reference ranges.

| Tumor marker | Normal value | Baseline (day 22) | After 2 cycles (~day 90) | After 4 cycles (~day 150) |
|---|---|---|---|---|
| CEA, ng/ml | <5.0 | 46.76 | 7.18 | 3.83 |
| CA125, U/ml | <35.0 | 108.10 | 11.20 | 9.30 |
| CYFRA21-1, ng/ml | <3.3 | 27.86 | 2.14 | 2.71 |
| SCC, ng/ml | <1.5 | 0.80 | 1.10 | 1.10 |
| NSE, ng/ml | <16.3 | 29.99 | 12.47 | 10.11 |

CEA, carcinoembryonic antigen; CA125, carbohydrate antigen 125; CYFRA21-1, cytokeratin 19 fragment; SCC, small cell carcinoma antigen; NSE, neuron specific enolase.

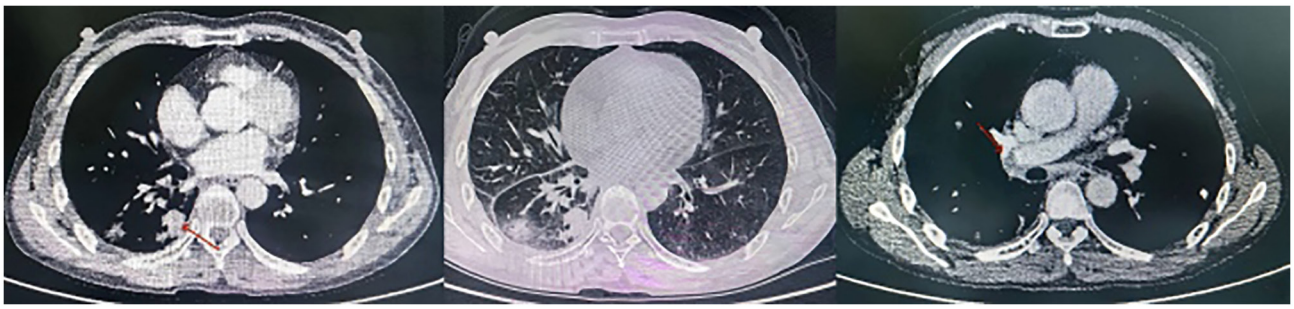


Figure 3. Chest computed tomography after 4 cycles of ivonescimab (June 2025), maintaining a partial response (47% reduction from baseline). Left panel: Continued regression of the primary lesion (arrow). Middle panel: Sustained improvement of pulmonary metastases. Right panel: Further reduction of the intrapulmonary primary lesion (arrow). Scanning parameters: 120 kV, 150 mAsec, 5-mm slice thickness. Scale bar, 1 cm.

pneumonitis. Pulmonary function tests revealed mild reductions in small airway function, with maximal mid-expiratory flow at 62% of predicted and maximal expiratory flow at 25% recorded at 65% of predicted, while forced expiratory volume in 1 sec (FEV1) and forced vital capacity (FVC) remained within normal limits (FEV1 89% of predicted, FVC 92% of predicted). After comprehensive evaluation, the diagnosis was Grade I (10) radiation pneumonitis (Fig. 5). Treatment included intravenous dexamethasone (5 mg on days 1-3), followed by sequential oral methylprednisolone starting at 20 mg/day, tapered by 4 mg every 3 days to a maintenance dose of 4 mg/day, then reduced by 2 mg every 3 days to discontinuation over a total of 4 weeks. Both imaging abnormalities and symptoms resolved within a short period. As of the last follow-up in August 2025, the patient had achieved 8 months of progression-free survival, with the ECOG PS score improving from a baseline of 2 points to 0 points, and a notable improvement in the quality of life.

## Discussion

The present case provides real-world evidence for the efficacy and safety of ivonescimab followed by consolidative

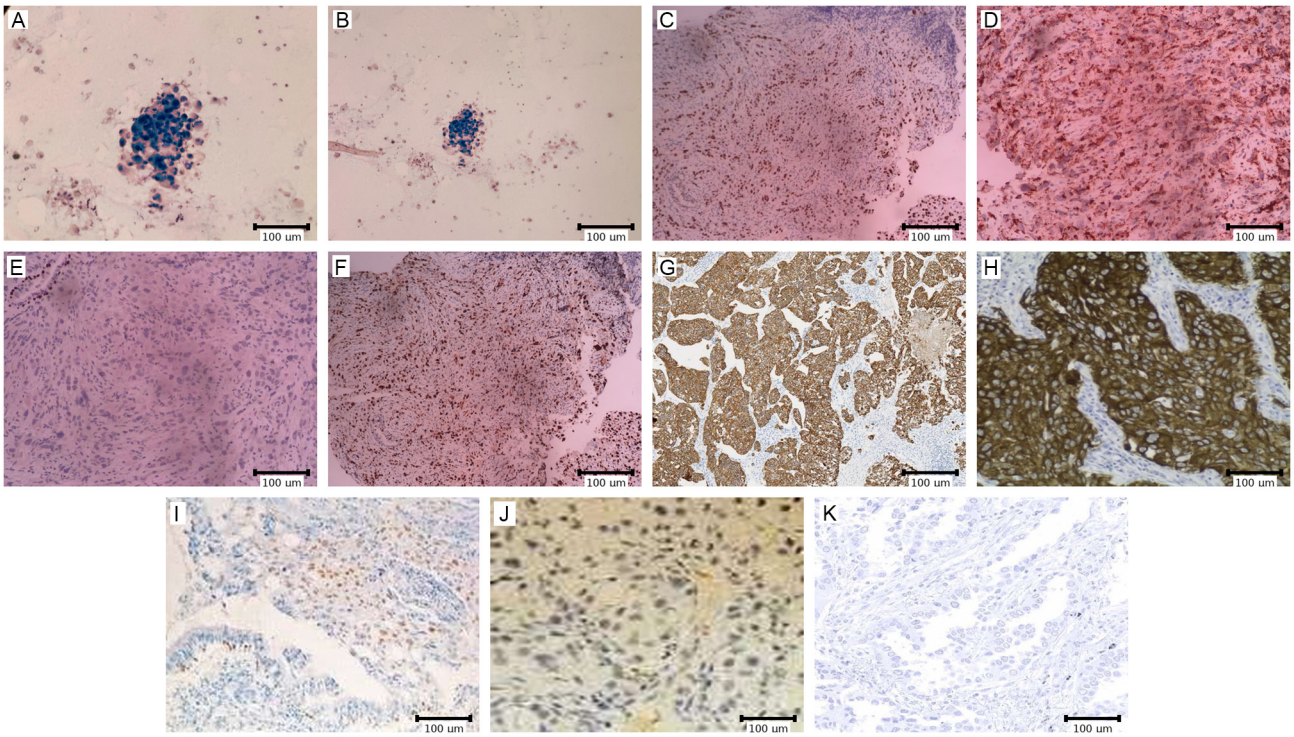



Figure 4. Histopathological and immunohistochemical findings of the lung biopsy specimen. (A and B) Hematoxylin and eosin-stained sections showing clusters of poorly differentiated adenocarcinoma cells (original magnification, x400; scale bar, 100 $\mu$m). (C) Thyroid transcription factor-1 positivity. (D) Napsin A positivity. (E) Negative expression of p40. (F) Negative expression of p63. (G) Pan-cytokeratin positivity. (H) CK7 positivity. (I) Loss of SMARCA4/BRG1 expression. (J) Negative expression of synaptophysin. (K) Ki-67 proliferation index of ~70%. [(C-K) Scale bar, 100 $\mu$m; original magnification, x400].

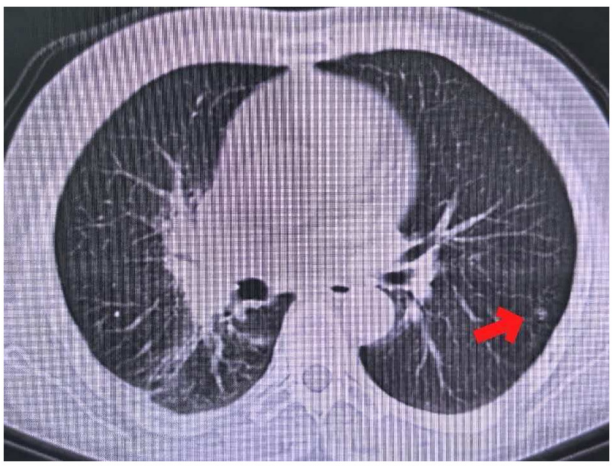


Figure 5. Chest computed tomography scan approximately 20 days after radiotherapy (July 2025) revealing stable primary lesions with new ground-glass opacities and linear opacities in the bilateral lungs (arrows), suggestive of radiation pneumonitis. Scanning parameters: 120 kV, 150 mAsec, 5-mm slice thickness.

radiotherapy in a patient with advanced lung adenocarcinoma exhibiting a PD-L1 TPS of 90% and a concurrent TP53 mutation. Several clinically relevant observations merit further discussion.

First, the depth of response observed with ivonescimab monotherapy in this 'super-responder' population is noteworthy. Following two cycles of treatment, the patient achieved a PR, with target lesion reduction reaching 47% after four cycles. This rapid and sustained tumor shrinkage aligns with findings from the phase III HARMONi-2 trial, which demonstrated superior progression-free survival with ivonescimab vs. pembrolizumab in patients with PD-L1 TPS ≥50% (4). In addition to imaging responses, serial monitoring of serum tumor markers, including CEA, CA125, CYFRA21-1 and NSE, revealed consistent decreases, further supporting the systemic antitumor activity of ivonescimab. These findings reinforce the potential of ivonescimab as a potent first-line option in advanced NSCLC with high PD-L1 expression.

Second, the sequential strategy of 'immunotherapy induction followed by radiotherapy consolidation' proved feasible and safe in the present case. After confirming a PR to four cycles of ivonescimab, the patient received thoracic intensity-modulated radiotherapy (50 Gy/25 fractions) for local consolidation. This approach was designed to leverage the synergistic potential of radiotherapy, including direct cytotoxicity, antigen release and enhancement of antitumor immunity, while minimizing the risk of overlapping toxicity. The patient developed only grade 1 radiation pneumonitis, which resolved rapidly with low-dose glucocorticoids. This favorable safety profile is consistent with the 2025 Chinese expert consensus, which supports the use of consolidative radiotherapy after effective systemic immunotherapy in selected patients with oligoresidual disease (10). Notably, this case illustrates that delaying radiotherapy until after an immunotherapy-induced response may optimize the therapeutic window and reduce the likelihood of severe immune-related adverse events. A recent comprehensive review by Burr *et al* (11) summarized the preclinical and clinical evidence for combining radiotherapy

with immunotherapy in NSCLC, concluding that the timing of these modalities is crucial to optimizing outcomes.

To contextualize the present findings, other case reports have described similar responses in NSCLC patients with high PD-L1 expression treated with sequential immunotherapy and radiotherapy. Xia *et al* (12) reported a case of lung adenocarcinoma with PD-L1 TPS ≥50% in which an extracranial abscopal effect was observed following brain radiotherapy alone, accompanied by a durable partial response to subsequent pembrolizumab therapy. This observation further supports the concept that radiotherapy can serve as an immunomodulator, even in the setting of high PD-L1 expression, whereby the abscopal effect may contribute to the efficacy of sequential strategies.

Several clinical factors may have influenced the treatment outcomes for the present patient. The patient had a baseline pulmonary infection that was treated with levofloxacin. This resolved before immunotherapy initiation and did not appear to affect the final response. The malignant pleural effusion was managed with intrapleural cisplatin plus bevacizumab, which likely contributed to local symptom control but is not known to exert systemic antitumor effects. The patient had no other comorbidities (diabetes, hypertension or autoimmune diseases), which could have confounded the safety profile.

The presence of a TP53 missense mutation in the present patient raises the possibility of a predictive biomarker for combined immunotherapy and radiotherapy. TP53 is the most frequently mutated gene in lung cancer and has been associated with increased tumor mutational burden, genomic instability and enhanced immunogenicity (13). Preclinical evidence suggests that p53 dysfunction may impair DNA damage repair, thereby increasing radiosensitivity, while also promoting immunogenic cell death via activation of the cyclic GMP-AMP synthase/stimulator of IFN genes pathway (14). In a cohort of 220 patients with metastatic non-squamous NSCLC, Mathiot *et al* (15) demonstrated that TP53 mutations were associated with significantly improved overall survival (24.7 vs. 12.0 months; P=0.017) and progression-free survival (9.6 vs. 3.2 months, P=0.048) times in patients receiving immune checkpoint inhibitor monotherapy. This finding is further corroborated by another large German cohort study of 696 patients with non-squamous NSCLC with high PD-L1 expression (≥50%) receiving first-line pembrolizumab monotherapy. Bischoff *et al* (16) demonstrated that patients with TP53 mutations, particularly when co-occurring with KRAS G12C mutations, experienced markedly longer progression-free survival (33.7 months) and overall survival (65.3 months) compared with those with wild-type TP53 (16). Notably, the improved outcomes were associated with a proinflammatory tumor microenvironment, characterized by high tumor-infiltrating lymphocyte densities and upregulation of IFNγ target genes (16). This large-scale, real-world evidence strongly supports the notion that TP53 mutations can be used to identify a subset of NSCLC patients with heightened sensitivity to immune checkpoint inhibitor monotherapy. In this context, the coexistence of high PD-L1 expression and TP53 mutation may have contributed to the deep and durable response observed in the present patient. Although hypothesis-generating, this case supports further investigation into TP53 mutation status as a potential biomarker for selecting candidates for combined modality approaches.

In summary, the present case highlights the clinical potential of a sequential regimen involving ivonescimab induction followed by consolidative radiotherapy in patients with advanced lung adenocarcinoma and high PD-L1 expression. The strategy achieved meaningful tumor regression, maintained quality of life (ECOG PS improved from 2 to 0) and demonstrated a manageable safety profile. Future prospective studies are warranted to validate optimal sequencing, fractionation schedules and biomarker-driven patient selection for this promising therapeutic approach.

In conclusion, for patients with advanced lung adenocarcinoma exhibiting high PD-L1 expression, a promising therapeutic strategy involves systemic treatment based on ivonescimab followed by sequential radical local radiotherapy after achieving marked efficacy. The combined data from this case and the HARMONi-2 study demonstrate that this strategy can induce a deep and durable tumor response in the favorable population, improve quality of life and maintain controllable safety, providing valuable reference for clinical practice.

**Acknowledgements**

Not applicable.

**Funding**

No funding was received.

**Availability of data and materials**

The data generated in the present study may be found in the NCBI Sequence Read Archive under accession number PRJNA1498320 or at the following URL: https://www.ncbi.nlm.nih.gov/bioproject/PRJNA1498320. The remaining data generated in the present study may be requested from the corresponding author.

**Authors' contributions**

QZ was responsible for the conceptualization and design of the study, the analysis and interpretation of clinical patient data, drafting the original manuscript, and reviewing and editing the final version. BY was responsible for the acquisition, review and interpretation of the clinical imaging data (CT scans and MRI) and pathological data to confirm the diagnosis (cT4N2bM1a), and for providing advice on patient treatment. HC was responsible for the acquisition and analysis of laboratory data (serum tumor markers), and the visualization of clinical figures and tables. JJ was responsible for designing the treatment protocol, providing clinical advice on systemic immunotherapy and radiotherapy, and supervising the treatment course. RC was responsible for conceptualization, critical revision of the manuscript for important intellectual content, and final approval of the version to be published. QZ and RC confirm the authenticity of all the raw data. All authors have read and approved the final manuscript.

**Ethics approval and consent to participate**

Not applicable.

## Patient consent for publication

Written informed consent was obtained from the patient for publication of this case report and any accompanying images.

## Competing interests

The authors declare that they have no competing interests.

## References


1. Zhou J, Xu Y, Liu J, Feng L, Yu J and Chen D: Global burden of lung cancer in 2022 and projections to 2050: Incidence and mortality estimates from GLOBOCAN. Cancer Epidemiol 93: 102693, 2024.
2. Hayashi H, Ogura M, Niwa T, Yokoyama T, Tanizaki J, Ozaki T, Yoshioka H, Kurata T, Tamura Y, Fujisaka Y, *et al*: Phase I/II study of cisplatin plus Nab-paclitaxel with concurrent thoracic radiotherapy for patients with locally advanced non-small cell lung cancer. Oncologist 26: 19-e52, 2021.
3. Dhillon S: Ivonescimab: First approval. Drugs 84: 1135-1142, 2024.
4. Xiong A, Wang L, Chen J, Wu L, Liu B, Yao J, Zhong H, Li J, Cheng Y, Sun Y, *et al*: Ivonescimab versus pembrolizumab for PD-L1-positive non-small cell lung cancer (HARMONi-2): A randomised, double-blind, phase 3 study in China. Lancet 405: 839-849, 2025.
5. Long R, Kuang W and Zhou Q: Ivonescimab plus chemotherapy in advanced or metastatic non-squamous non-small cell lung cancer with EGFR variant in China: A cost-effectiveness analysis. Transl Lung Cancer Res 14: 1622-1634, 2025.
6. Al Matairi A, Hammadeh BM, Aldalati AY, Qtaishat FA, Nashwan AJ and Alzibdeh A: Efficacy and safety of ivonescimab in the treatment of advanced non-small cell lung cancer (NSCLC): A systematic review. Cureus 17: e77381, 2025.
7. Karcioglu O, Topacoglu H, Dikme O and Dikme O: A systematic review of the pain scales in adults: Which to use? Am J Emerg Med 36: 707-714, 2018.
8. Oken MM, Creech RH, Tormey DC, Horton J, Davis TE, McFadden ET and Carbone PP: Toxicity and response criteria of the eastern cooperative oncology group. Am J Clin Oncol 5: 649-655, 1982.
9. Detterbeck FC, Boffa DJ, Kim AW and Tanoue LT: The eighth edition lung cancer stage classification. Chest 151: 193-203, 2017.
10. Multidisciplinary Committee on Oncology, Chinese Medical Doctor Association; Expert Committee on Quality Control of Lung Cancer, National Quality Control Center for Cancer: Chinese expert consensus on the combination of immune checkpoint inhibitors and radiotherapy for lung cancer (2025 edition). Zhonghua Zhong Liu Za Zhi 47: 39-64, 2025 (In Chinese).
11. Burr JL, Johnson KC, Carmicheal JJ, Lin C and Ganti AK: Combination Immunotherapy with radiotherapy in non-small cell lung cancer: A review of evidence. Cancer Med 13: e70402, 2024.
12. Xia Y, Zhu H, Huang S, Guan X, Chen X, Zhang Q, Meng L, Xue H, Xiang H, Lai S and Lou J: Remarkable response to pembrolizumab in PD-L1 overexpressing (≥ 50%) NSCLC and extracranial abscopal effect induced by brain radiotherapy: A case report. Front Oncol 15: 1652515, 2025.
13. Li L, Li M and Wang X: Cancer type-dependent correlations between TP53 mutations and antitumor immunity. DNA Repair (Amst) 88: 102785, 2020.
14. Ghosh M, Saha S, Li J, Montrose DC and Martinez LA: p53 engages the cGAS/STING cytosolic DNA sensing pathway for tumor suppression. Mol Cell 83: 266-280.e6, 2023.
15. Mathiot L, Nigen B, Goronflot T, Hiret S, Doucet L, Pons-Tostivint E, Bennouna J, Denis MG, Herbreteau G and Raimbourg J: Prognostic impact of TP53 mutations in metastatic nonsquamous non-small-cell lung cancer. Clin Lung Cancer 25: 244-253.e2, 2024.
16. Bischoff P, Reck M, Overbeck T, Christopoulos P, Rittmeyer A, Lüders H, Kollmeier J, Kulhavy J, Kemper M, Reinmuth N, *et al*: Outcome of first-line treatment with pembrolizumab according to KRAS/TP53 mutational status for nonsquamous programmed death-ligand 1-high (≥50%) NSCLC in the German national network genomic medicine lung cancer. J Thorac Oncol 19: 803-817, 2024.


Copyright © 2026 Zhou et al. This work is licensed under a Creative Commons Attribution-NonCommercial-NoDerivatives 4.0 International (CC BY-NC-ND 4.0) License.